Infectious Disease Modelling 2 (2017) 21–34

Contents lists available at ScienceDirect

Infectious Disease Modelling

journal homepage: www.keaipublishing.com/idm

Role of short-term dispersal on the dynamics of Zika virus in an extreme idealized environment

Victor M. Moreno [a, *], Baltazar Espinoza [a], Derdei Bichara [a, d], Susan A. Holechek [a, b, c], Carlos Castillo-Chavez [a, e, f]

[a] Simon A. Levin Mathematical, Computational and Modeling Sciences Center, Arizona State University, P.O. Box 873901, Tempe, AZ 85287-3901, United States
[b] Biodesign Center for Infectious Diseases and Vaccinology, Biodesign Institute, Arizona State University, Tempe, AZ 85287-5401, United States
[c] School of Life Sciences, Arizona State University, Tempe, AZ 85287-4501, United States
[d] Department of Mathematics and Center for Computational and Applied Mathematics, California State University, Fullerton, CA 92831, United States
[e] Departamento the Ingenieria Biomedica, Universidad de Los Andes, Bogota, Colombia
[f] Rector's Office, Yachay Tech University, Urcuqui, Ecuador

ARTICLE INFO

Article history:
Received 14 December 2016
Accepted 14 December 2016
Available online 19 December 2016

Keywords:
Vector-borne diseases
Zika virus
Residence times
Multi-patch model

ABSTRACT

In November 2015, El Salvador reported their first case of Zika virus (ZIKV) infection, an event followed by an explosive outbreak that generated over 6000 suspected cases in a period of two months. National agencies began implementing control measures that included vector control and recommending an increased use of repellents. Further, in response to the alarming and growing number of microcephaly cases in Brazil, the importance of avoiding pregnancies for two years was stressed. In this paper, we explore the role of mobility within communities characterized by extreme poverty, crime and violence. Specifically, the role of short term mobility between two idealized interconnected highly distinct communities is explored in the context of ZIKV outbreaks. We make use of a Lagrangian modeling approach within a two-patch setting in order to highlight the possible effects that short-term mobility, within *highly distinct* environments, may have on the dynamics of ZIKV outbreak when the overall goal is to reduce the number of cases not just in the most affluent areas but everywhere. Outcomes depend on existing mobility patterns, levels of disease risk, and the ability of federal or state public health services to invest in resource limited areas, particularly in those where violence is systemic. The results of simulations in highly polarized and simplified scenarios are used to assess the role of mobility. It quickly became evident that matching observed patterns of ZIKV outbreaks could not be captured without incorporating increasing levels of heterogeneity. The number of distinct patches and variations on patch connectivity structure required to match ZIKV patterns could not be met within the highly aggregated model that is used in the simulations.

© 2016 KeAi Communications Co., Ltd. Production and hosting by Elsevier B.V. This is an open access article under the CC BY-NC-ND license (http://creativecommons.org/licenses/by-nc-nd/4.0/).

* Corresponding author.
E-mail address: vmmoren4@asu.edu (V.M. Moreno).
Peer review under responsibility of KeAi Communications Co., Ltd.

http://dx.doi.org/10.1016/j.idm.2016.12.002
2468-0427/© 2016 KeAi Communications Co., Ltd. Production and hosting by Elsevier B.V. This is an open access article under the CC BY-NC-ND license (http://creativecommons.org/licenses/by-nc-nd/4.0/).

1. Introduction

Zika virus (ZIKV), an emerging mosquito-borne flavivirus related to yellow fever, dengue, West Nile and Japanese encephalitis (Hayes et al, 2009), has taken the Americas by storm. ZIKV is transmitted primarily by *Aedes aegypti* mosquitoes, which also transmit dengue and chikungunya. As of February 9, 2016, according to the CDC (CDC(a), 2016), ZIKV cases had been reported throughout the Caribbean, Mexico and South America with the exception of Chile, Uruguay, Argentina, Paraguay and Peru. Several states within the United States had also reported ZIKV cases (Petersen, 2016) and although it is expected that ZIKV will be managed effectively within the USA, the possibility of localized ZIKV outbreaks has yet to be ruled out.

Phylogenetic analyses have revealed the existence of two main virus lineages (African and Asian) (Faye et al., 2014; Haddow et al., 2012) albeit so far, no concise clinical differences have been identified between infections with strains from these lineages. Further, the reports are not surprising since most African samples come from a rhesus sentinel in Uganda, where ZIKV was first discovered, during primate and mosquito surveillance efforts aimed at assessing Yellow Fever trends in 1947 (Dick, Kitchen, & Haddow, 1952). The African lineage has circulated primarily in wild primates and arboreal mosquitoes such as *Aedes africanus* within a specific geographic habitat; a narrow equatorial belt running across Africa and into Asia. Spillover infections in humans have rarely occurred even in areas found to be highly enzootic (Fauci & Morens, 2016; Musso, Cao-Lormeau, & Gubler, 2015). The Asian lineage, which seems to have originated from the adaptation of the virus as it successfully invaded a different vector, *Aedes aegypti*, a variant capable of infecting human populations rather effectively, (Fauci & Morens, 2016; Haddow et al., 2012), is the dominant type in the Americas.

The first human infection was reported in Nigeria in 1954 (Macnamara, 1954). The evidence of when ZIKV moved out of Africa and Asia was provided by the 2007 outbreak in Yap Island in the Federated States of Micronesia (Duffy et al., 2009); an outbreak followed by larger outbreak in French Polynesia in 2013–2014 (Cao-Lormeau & Musso, 2014). The virus then appeared in New Caledonia, the Cook Islands and Eastern Islands (Musso, Nilles, & Cao-Lormeau, 2014). Decades old data from African researchers seem to support the possibility that ZIKV spread may have been facilitated by prior chikungunya epizootics (Fauci & Morens, 2016). If this is the case then the pattern seemed to have repeated itself in 2013 when chikungunya spread from west to east, a sequence of outbreaks followed by ZIKV outbreaks (Fauci & Morens, 2016).

In early 2015, ZIKV was detected in Brazil. Phylogenetic analyses of the virus isolated from patients, placed the Brazilian strains within the Asian lineage (Zanluca et al., 2015); that is, the one previously detected during the French Polynesian outbreak (Cao-Lormeau et al., 2014). Since the first detection of ZIKV in Brazil, we have seen its range to grow reaching rather quickly the nations of Bolivia, Brazil, Colombia, Ecuador, French Guyana, Guyana, Paraguay, Suriname and Venezuela (CDC(c), 2016). Furthermore, several Central America countries have now been invaded by the ZIKV, including Costa Rica, El Salvador, Guatemala, Honduras, Nicaragua and Panama (CDC(d), 2016). As of September 23, 2016, all of the nations in the Americas have experience active ZIKV outbreaks with the exception of Canada, Chile and Uruguay (CDC(f), 2016). The rapid geographic expansion of ZIKV has led the World Health Organization (WHO) to declare it an international public health emergency (W. H. O. (WHO), 2016).

It has been estimated that about 80% of people infected with ZIKV are asymptomatic (Zika virus, 2016; Duffy et al., 2009) in line with various vector born diseases spread by *Aedes aegypti* mosquitoes. ZIKV clinical manifestations include dengue-like symptoms, that is, arthralgia, particularly swelling, mild fever, lymphadenopathy, skin rash, headaches, retro orbital pain, and conjunctivitis, which normally last for 2–7 days (Zika virus, 2016; W. H. O. (WHO), 2016; Zanluca et al., 2015). The similarities in symptoms, sources of mis-identification, bring a high level of uncertainty in efforts to asses the number of patients infected with ZIKV. It is believe that it may be higher than what it has been reported (Fauci & Morens, 2016; Salvador & Fujita, 2015). Moreover, for example, co-infection with dengue and ZIKV is not uncommon and as a result ZIKV diagnosis is difficult (Dupont-Rouzeyrol et al., 2015).

At present, there is no ZIKV vaccine available. Further, ZIKV infections are being linked with neurological (microcephaly) and auto-immune (Guillain-Barré syndrome) complications. Evidence supports a troubling new transmission mode for a vector born disease, namely that of sexual transmission (CDC(b), 2016; W. H. O. (WHO), 2016). Education on ZIKV modes of transmission and ways of preventing transmission are essential to halt ZIKV spread at regional, national and global levels. Control measures are limited and include the use of insect repellents to the use of protection while engaged in sexual activity and sex abstinence (CDC(b), 2016). An inexpensive effective way to diagnose ZIKV seems to have been found. Scientists from Arizona State University and Harvard University have created a diagnostic tool, similar to a pregnancy test, capable of given a quick, effective, simple and inexpensive way of diagnosing ZIKV infections (Gazette, 2016; The Biodesign Institute, 2016).

Resource limited and poor nations face challenges that make the use of standard efforts and approaches aimed at controlling vector borne diseases ineffective due to extreme variations in the levels of public safety, gang violence and conflict. A lack of attention to the threats posed by the weakest links in the global spread of diseases poses a serious threat to global health policies (see (Castillo-Chavez et al., 2015; Chowell, Castillo-Chavez, Krishna, Qiu, & Anderson, 2015; Espinoza, Moreno, Bichara, & Castillo-Chavez, 2016, p. pp.123; Patterson-Lomba, Goldstein, Gómez-Liévano, Castillo-Chavez, & Towers, 2015, 2016, p. pp.1011; Perrings et al., 2014; Zhao, Feng, & Castillo-Chavez, 2014)). The

importance of focusing on the weakest links of global transmission networks becomes obvious when the levels of violence in Latin America and the Caribbean, which houses 9% of the global population but accounts for 33% of the world's homicides (Jaitman, 2015). In this study, we analyze the impact that restrictions to public safety, which affect mobility and altered the levels of local risk, may have on the dynamics of ZIKV transmission and control. The long-term interest of our efforts is to limit the role that violence and conflict play on the overall health patterns of individuals living in the Caribbean, particularly in El Salvador.

2. Single patch model

We revisit a simplified vector-borne transmission model, a building block for the derivation of *highly simplified* two-patch scenarios. Two-patch models are used to explore the role of residence times and risk (possibly defined by underlying levels of violence or a lack of a health-medical infrastructure) on the dynamics of the ZIKV. The general version of an N-patch framework and its analysis can be found in (Bichara & Castillo-Chavez, 2016).

Patch heterogeneity is built in by assuming that within the first patch there is low levels of security making it difficult to carry out sustainable vector control efforts. The second patch is considered to be safe with its population having access to reasonable health services on demand. In other words, we are focusing on a highly bi-modal situation, an idealized situation that does not capture the levels of complexity and heterogeneity present in conflict or crime ridden communities.

Simulations based on highly idealized exploratory settings may lead to more credible conclusions if the models are parameterized using “realistic” estimates of the parameters involved. Highly detailed models, for example, agent based models, require huge amounts of data as well as the type information that often has still to be collected or measured within accepted protocols. The proper parametrization of detailed models may require detailed accounts of individuals' daily mobility activities as it was done, for example, by those working on the EpiSims project (Stroud, Del Valle, Sydoriak, Riese, & Mniszewski, 2007); the kind of worthwhile far reaching project that we hope that this paper may instigate in the context of communities where violence and health disparities are the norm.

Within this manuscript, it is assumed that each patch is made up of individuals experiencing the same degree of risk of infection, which is just a function of the patch. Consequently, all individuals while in Patch 1 will be experiencing high risk of infection while those in Patch 2 will be experiencing low risk. In short, movement (daily activities) would alter the amount of time that each individual spends on each patch, the longer that an individual is found in Patch 1, the more likely that he/she will become infected. The level of patch-specific risk to infection is captured via the use of a single parameter $\widehat{\beta}_i$, $i = 1, 2$ with $\widehat{\beta}_1 \gg \widehat{\beta}_2$. This assumption models in a rather simplistic way the health disparities that we address within a highly polarized setting. This is a first effort aimed at exploring the role of risk and mobility on the dynamics of ZIKV in a world where two highly-distinct mobile communities co-exist. The case of Johannesburg and Soweto in South Africa, or North and South Bogota in Colombia, or Rio de Janeiro and adjacent favelas in Brazil, or gang-controlled and gang-free areas within San Salvador, are but some of the unfortunately large number of pockets dominated by conflict or high crime within urban centers around world. The short time scale dynamics of individuals (daily mobility as they go to work or carry out on other activities including attendance to schools and universities) in both patches are incorporated within this model with the analysis (simulations) carried out over the duration of a *single* outbreak.

The ZIKV dynamics single patch model involves hosts and vectors populations of size N_h and N_v. Both populations are subdivided by epidemiological states; the transmission process is modeled as the result of the interactions of these populations. On that account, we let S_h, E_h, $I_{h,a}$, $I_{h,s}$ and R_h denote the susceptible, latent, infectious asymptomatic, infectious symptomatic and recovered host sub-populations. Similarly, S_v, E_v and I_v are used to denote the susceptible, latent and infectious mosquito sub-populations. Since the focus is on the study of disease dynamics over a single outbreak, we neglect the hosts' demographics while assuming that the vector's demographics do not change, meaning that, it is assumed the birth and death per capita mosquito rates cancel each other out. New reports (Zika virus, 2016; Duffy et al., 2009) point out the presence of large numbers of asymptomatic ZIKV infectious individuals. Consequently, we consider two classes of infectious $I_{h,a}$ and $I_{h,s}$, that is, asymptomatic and symptomatic infectious individuals. Further, since there is no full knowledge of the dynamics of ZIKV transmission, it is assumed that $I_{h,a}$ and $I_{h,s}$ individuals are equally infectious with their periods of infectiousness roughly the same. Our assumptions could be used to reduce the model to one that considers a single infectious class $I_h = I_{h,a} + I_{h,s}$. We keep both infectious classes as it may be desirable to keep track of each type. These assumptions may not be too bad given our current knowledge of ZIKV epidemiology and the fact that ZIKV infections, in general, are not severe. Furthermore, given that the infectious process of ZIKV is somewhat similar to that of dengue, we use some of the parameters estimated in dengue transmission studies within El Salvador. ZIKV basic reproduction number estimates are taken from those that we just estimated using outbreak data from Barranquilla Colombia (Towers et al., 2016). Furthermore, the selection of model parameters ranges used, also benefited from prior estimates conducted with data from the 2013–2014 French Polynesia outbreak (Kucharski et al., 2016), some of the best available. The dynamics of the prototypic single patch system, single epidemic outbreak, can therefore modeled using the following standard nonlinear system of differential equations (Brauer & Castillo-Chavez, 2012):

$$\begin{cases} \dot{S}_h = -b\beta_{vh}S_h\dfrac{I_v}{N_h} \\ \dot{E}_h = b\beta_{vh}S_h\dfrac{I_v}{N_h} - \nu_h E_h \\ \dot{I}_{h,s} = (1-q)\nu_h E_h - \gamma_h I_{h,s} \\ \dot{I}_{h,a} = q\nu_h E_h - \gamma_h I_{h,a} \\ \dot{R}_h = \gamma_h(I_{h,s} + I_{h,a}) \\ \dot{S}_v = \mu_v N_v - b\beta_{hv}S_v\dfrac{I_{h,s}+I_{h,a}}{N_h} - \mu_v S_v \\ \dot{E}_v = b\beta_{hv}S_v\dfrac{I_{h,s}+I_{h,a}}{N_h} - (\mu_v+\nu_v)E_v \\ \dot{I}_v = \nu_v E_v - \mu_v I_v \end{cases} \tag{1}$$

The parameters of Model 1 are collected and described in Table 1 while the model flow diagram is presented in Fig. 1.

The *basic reproduction number* for this prototypic model, that is, the average number of secondary infections generated by a typical infectious individual in a population where nobody has experienced a ZIKV-infection is computed by taking $S(0) = N_h$ in Model (1). The basic reproduction number is given by

$$\begin{aligned} \mathscr{R}_0^2 &= \frac{b^2 N_v \beta_{vh}\beta_{hv}\nu_v[(1-q)\gamma_h + q\gamma_h]}{N_h\gamma_h^2\mu_v(\mu_v+\nu_v)} \\ &:= \mathscr{R}_{0,s}^2 + \mathscr{R}_{0,a}^2. \\ \mathscr{R}_0 &= \sqrt{\frac{N_v b^2\beta_{vh}\beta_{hv}\nu_v}{N_h\gamma_h\mu_v(\nu_v+\mu_v).}} \end{aligned} \tag{2}$$

The reduced form corresponds to the basic reproduction number when $I_h = I_{h,a} + I_{h,s}$.

The dynamics of the single patch model are well known. In short, if $\mathscr{R}_0 \leq 1$, there is no epidemic outbreak, that is, the proportion of introduced infected individuals decrease, while if $\mathscr{R}_0 > 1$ we have that the infected host population grows, an outbreak takes place, that is, the number of cases exceeds the initial size of the introduced infected population at time $t = 0$. Finally, when $\mathscr{R}_0 > 1$, the population of infected individuals eventually decreases and the disease dies out (single outbreak model).

In the next section, a two patch model using the Lagrangian approach specified in (Bichara & Castillo-Chavez, 2016; Bichara, Kang, Castillo-Chavez, Horan, & Perrings, 2015) is introduced with individuals from Patch i ($i = 1, 2$) never loosing their residency status as a result of their daily mobility patterns across patches; an assumption captured with the use of a *residence time matrix*. A matrix, where each entry p_{ij} models the average (fixed) proportion of time that a typical resident spends on his/her own patch or as a visitor to another patch per unit of time, hence ($p_{i1} + p_{i2} = 1$). Hence, at any given time t, the effective population size in each patch does not necessarily match that given by the number of patch residents. In our framework, we make sure that *population patch size at time t* does account for patch residents (in residency at time t) and patch visitors in *at time t*.

Table 1
Description of the parameters used in System (1).

Parameters	Description	Value
β_{vh}	Infectiousness of human to mosquitoes	0.41
β_{hv}	Infectiousness of mosquitoes to humans	0.5
b_i	Biting rate in Patch i	0.8
ν_h	Humans' incubation rate	$\frac{1}{7}$
q	Fraction of latent that become asymptomatic and infectious	0.1218
γ_i	Recovery rate in Patch i	$\frac{1}{5}$
p_{ij}	Proportion of time residents of Patch i spend in Patch j	$[0, 1]$
μ_v	Vectors' natural mortality rate	$\frac{1}{13}$
ν_v	Vectors' incubation rate	$\frac{1}{9.5}$

3. Residence times and two-patch models

The role of mobility between two communities, within the same city, living under dramatically distinct health, economic, social and security settings is explored using a model as *simple* as possible, that is, a model that only considers two patches (prior modeling efforts that didn't account for the effective population size but that incorporated specific controls include, (Lee & Castillo-Chavez, 2015)). It is assumed that Patch 2 has access to working health facilities, low crime rate, adequate human and financial resources and adequate public health policies, in place. On the other hand, Patch 1 lacks nearly everything and crime is high. Within this highly simplified setting, the differences in risk naturally, which depend on host vector ratios, biting rates, the level of access and ability to buy repellents and nets, the regularity of visits by vector control crews and more, need to be incorporated. These differences are captured by just postulating *highly distinct transmission rates*; that is, we study the dynamics of host mobility in highly distinct environments, with risk being captured by the transmission rate, $\widehat{\beta}$. Hence, $\widehat{\beta_1} \gg \widehat{\beta_2}$ where $\widehat{\beta_i}$ defines the risk in Patch i, $i = 1, 2$ [Patch 1 (high risk) and Patch 2 (low risk)].

The host populations are stratified by epidemiological classes indexed by the patch of residence. Particularly $S_{h,i}$, $E_{h,i}$, $I_{h,a,i}$, $I_{h,s,i}$ and $R_{h,i}$ denote the susceptible, latent, infectious asymptomatic, infectious symptomatic and recovered host populations in patch i, $i = 1, 2$ with $S_{v,i}$, $E_{v,i}$ and $I_{v,i}$ denoting the susceptible, latent and infectious mosquito populations in patch i, $i = 1, 2$. As before, $N_{h,i}$ denotes the host patch population size $(i, i = 1, 2)$ and $N_{v,i}$ the total vector population in patch i, $i = 1, 2$. The vector is assumed to be incapable of moving between patches; a reasonable assumption in the case of *Aedes aegypti* under the appropriate spatial scale. The patch model-parameters are collected in Table 1 with the flow diagram, single-patch dynamics model, capturing the situation when residents and visitors do not move; that is, when the 2×2 residence times matrix $\mathbb{P}$ is such that $p_{11} = p_{22} = 1$ (Fig. 1).

3.1. Two patch model

The Lagrangian framework, in the context of vector born and communicable diseases, is described in (Bichara & Castillo-Chavez, 2016; Bichara et al., 2015, 2016). The application of this framework within a two patch model setting, where vectors are incapable of moving across patches, leads to the following set of nonlinear differential equations:

$$\begin{cases} \dot{S}_{h,i} = -\beta_{vh} S_{h,i} \sum_{j=1}^{2} b_j p_{ij} \dfrac{I_{v,j}}{p_{1j}N_{h,1} + p_{2j}N_{h,2}} \\ \dot{E}_{h,i} = \beta_{vh} S_{h,i} \sum_{j=1}^{2} b_j p_{ij} \dfrac{I_{v,j}}{p_{1j}N_{h,1} + p_{2j}N_{h,2}} - \nu_{h,i} E_{h,i} \\ \dot{I}_{h,s,i} = (1-q)\nu_{h,i} E_{h,i} - \gamma_{h,s} I_{h,s,i} \\ \dot{I}_{h,a,i} = q\nu_{h,i} E_{h,i} - \gamma_{h,a} I_{h,a,i} \\ \dot{R}_{h,i} = \gamma_{h,s} I_{h,s,i} + \gamma_{h,a} I_{h,a,i} \\ \dot{S}_{v,i} = \mu_v N_{v,i} - b_i \beta_{hv} S_{v,i} \dfrac{\sum_{j=1}^{2} p_{ji} \left(I_{h,s,j} + I_{h,a,j} \right)}{\sum_{k=1}^{2} p_{ki} N_{h,k}} - \mu_v S_{v,i} \\ \dot{E}_{v,i} = b_i \beta_{hv} S_{v,i} \dfrac{\sum_{j=1}^{2} p_{ji} \left(I_{h,s,j} + I_{h,a,j} \right)}{\sum_{k=1}^{2} p_{ki} N_{h,k}} - (\mu_v + \nu_v) E_{v,i} \\ \dot{I}_{v,i} = \nu_v E_{v,i} - \mu_v I_{v,i} \end{cases} \tag{3}$$

The basic reproduction number of this model is the largest eigenvalue of the matrix,

$$M_1 = \begin{pmatrix} m_{11} & m_{12} \\ m_{21} & m_{22} \end{pmatrix}$$

where

$$\begin{aligned} m_{11} &= \frac{p_{11}^2 N_{v,1} N_{h,1} b_1^2 \beta_{vh} \beta_{hv} \nu_v + p_{21}^2 N_{v,1} N_{h,2} b_1^2 \beta_{vh} \beta_{hv} \nu_v}{\left(p_{11}N_{h,1} + p_{21}N_{h,2}\right)^2 \gamma_h \mu_v (\nu_v + \mu_v)} \\ &= \left(\frac{p_{11}^2 N_{h,1} + p_{21}^2 N_{h,2}}{\left(p_{11}N_{h,1} + p_{21}N_{h,2}\right)^2} \right) \left(\frac{N_{v,1} b_1^2 \beta_{vh} \beta_{hv} \nu_v}{\gamma_h \mu_v (\nu_v + \mu_v)} \right), \end{aligned}$$

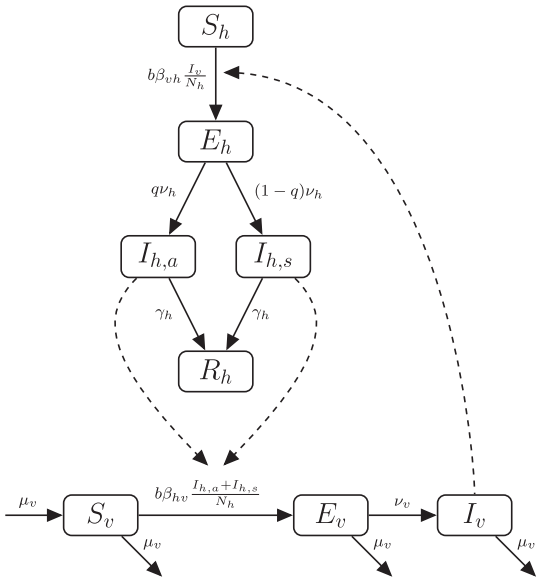

Fig. 1. Flow diagram of the model.

$$
\begin{aligned}
m_{12} &= \frac{p_{11}p_{12}N_{v,1}N_{h,1}b_1b_2\beta_{vh}\beta_{hv}\nu_v + p_{21}p_{22}N_{v,1}N_{h,2}b_1b_2\beta_{vh}\beta_{hv}\nu_v}{(p_{11}N_{h,1}+p_{21}N_{h,2})(p_{12}N_{h,1}+p_{22}N_{h,2})\gamma_h\mu_v(\nu_v+\mu_v)} \\
&= \left(\frac{p_{11}p_{12}N_{h,1}+p_{21}p_{22}N_{h,2}}{(p_{11}N_{h,1}+p_{21}N_{h,2})(p_{12}N_{h,1}+p_{22}N_{h,2})}\right)\left(\frac{N_{v,1}b_1b_2\beta_{vh}\beta_{hv}\nu_v}{\gamma_h\mu_v(\nu_v+\mu_v)}\right), \\
m_{21} &= \frac{p_{11}p_{12}N_{v,2}N_{h,1}b_1b_2\beta_{vh}\beta_{hv}\nu_v + p_{21}p_{22}N_{v,2}N_{h,2}b_1b_2\beta_{vh}\beta_{hv}\nu_v}{(p_{11}N_{h,1}+p_{21}N_{h,2})(p_{12}N_{h,1}+p_{22}N_{h,2})\gamma_h\mu_v(\nu_v+\mu_v)} \\
&= \left(\frac{p_{11}p_{12}N_{h,1}+p_{21}p_{22}N_{h,2}}{(p_{11}N_{h,1}+p_{21}N_{h,2})(p_{12}N_{h,1}+p_{22}N_{h,2})}\right)\left(\frac{N_{v,2}b_1b_2\beta_{vh}\beta_{hv}\nu_v}{\gamma_h\mu_v(\nu_v+\mu_v)}\right). \\
m_{22} &= \frac{p_{12}^2N_{v,2}N_{h,1}b_2^2\beta_{vh}\beta_{hv}\nu_v + p_{22}^2N_{v,2}N_{h,2}b_2^2\beta_{vh}\beta_{hv}\nu_v}{(p_{12}N_{h,1}+p_{22}N_{h,2})^2\gamma_h\mu_v(\nu_v+\mu_v)} \\
&= \left(\frac{p_{12}^2N_{h,1}+p_{22}^2N_{h,2}}{(p_{12}N_{h,1}+p_{22}N_{h,2})^2}\right)\left(\frac{N_{v,2}b_2^2\beta_{vh}\beta_{hv}\nu_v}{\gamma_h\mu_v(\nu_v+\mu_v)}\right).
\end{aligned}
$$

Specifically, we have that,

$$
\mathscr{R}_0^2 = \frac{1}{2}\left(m_{11}+m_{22}+\sqrt{(m_{11}-m_{22})^2-4m_{12}m_{21}}\right).
$$

If the two patches are isolated, a case that allows us to estimate the power of ZIKV transmission when each community deals with ZIKV independently then local basic reproduction number is $\mathscr{R}_0 = \max\{\mathscr{R}_{0i}\}$, $i = 1, 2$, where,

$$
\mathscr{R}_{0i} = \sqrt{\frac{N_{v,i}b_i^2\beta_{vh}\beta_{hv}\nu_v}{N_{h,i}\gamma_h\mu_v(\nu_v+\mu_v)}}
$$

that is, the expression found in Formula (2), with patch risk disparity, captured via the inequality, $\widehat{\beta_1} \gg \widehat{\beta_2}$, which turns out to be directly proportional to the local basic reproduction numbers ($\mathscr{R}_{0i}$) in the absence of mobility (uncoupled patches). Changes in the entries of the coupling matrix $\mathbb{P}$, would naturally impact the (two-patch) global basic reproduction number, $\mathscr{R}_0$ and, the dynamics of ZIKV on the overall two-patch system, including the final epidemic size and the ZIKV levels of infection within each patch. We then proceed to collect the results of a series of observations based on the simulation of

extreme scenarios, all designed to explore the role that mobility ($\mathbb{P}$), variations in patch risk ($\mathscr{R}_{0i}$) and population density on the risk and impact of a ZIKV outbreak on each patch. Naturally, the use of an extreme and simplistic set up is unlikely to yield a broad characterization of the role of mobility, variations in risk and host density on ZIKV outbreaks within heterogenous populations. Simulation results highlight nevertheless the impact that mobility, necessary for our economic survival (Soweto residents working primarily in Johannesburg, South Africa), has on ZIKV outbreaks; or the impact of high levels of crime and the restrictions that it imposes on vector borne control interventions (San Salvador, Rio de Janeiro and others) on ZIKV outbreaks. The upshot is that the sharing of health and security resources between resource-rich and resource-limited *adjacent* communities can make a difference whenever there is an agreement on the tradeoffs between public good and individual safety.

4. Results

The impact of risk and mobility under few selected, non exhaustive, scenarios is used to highlight the impact of mobility and risk under our restricted bi-modal set up. As specified, Patch 1 experiences high levels of crime, poverty and lack of resources while Patch 2 has access to vector control measures, health care facilities and resources to minimize local crime and violence; scenarios motivated by the dynamics of disease in conflict zones.

Since individuals experience a higher risk of ZIKV infection while in Patch 1 then it is assumed that mobility from Patch 2 to Patch 1 is unappealing with typical Patch 2 residents spending (on the average) a reduced amount of time each unit of time in Patch 1. Parameters are chosen so that the dynamics of ZIKV within Patch 2 cannot be supported in the absence of mobility between Patch 1 and Patch 2. Thus, the Patch 2 local basic reproductive number is taken to be less than one, namely, $\mathscr{R}_{02} = 0.9$. Mobility is modeled under the residence times matrix $\mathbb{P}$ with entries given *initially* by, $p_{21} = 0.10$ and $p_{12} = 0$.

Two cases are explored: A "worst case" scenario where control measures are hardly implemented due to crime, conflict or other factors on Patch 1, that is, Patch 1 is a place where the risk of acquiring a ZIKV infection is high since $\mathscr{R}_{01} = 2$. The "best case" scenario corresponds to the case when Patch 1 can implement some control measures with some degree of effectiveness and, consequently Patch 1 has an $\mathscr{R}_{01} = 1.52$. The $\mathscr{R}_{0i}$ values use are in line with those previously estimated for ZIKV

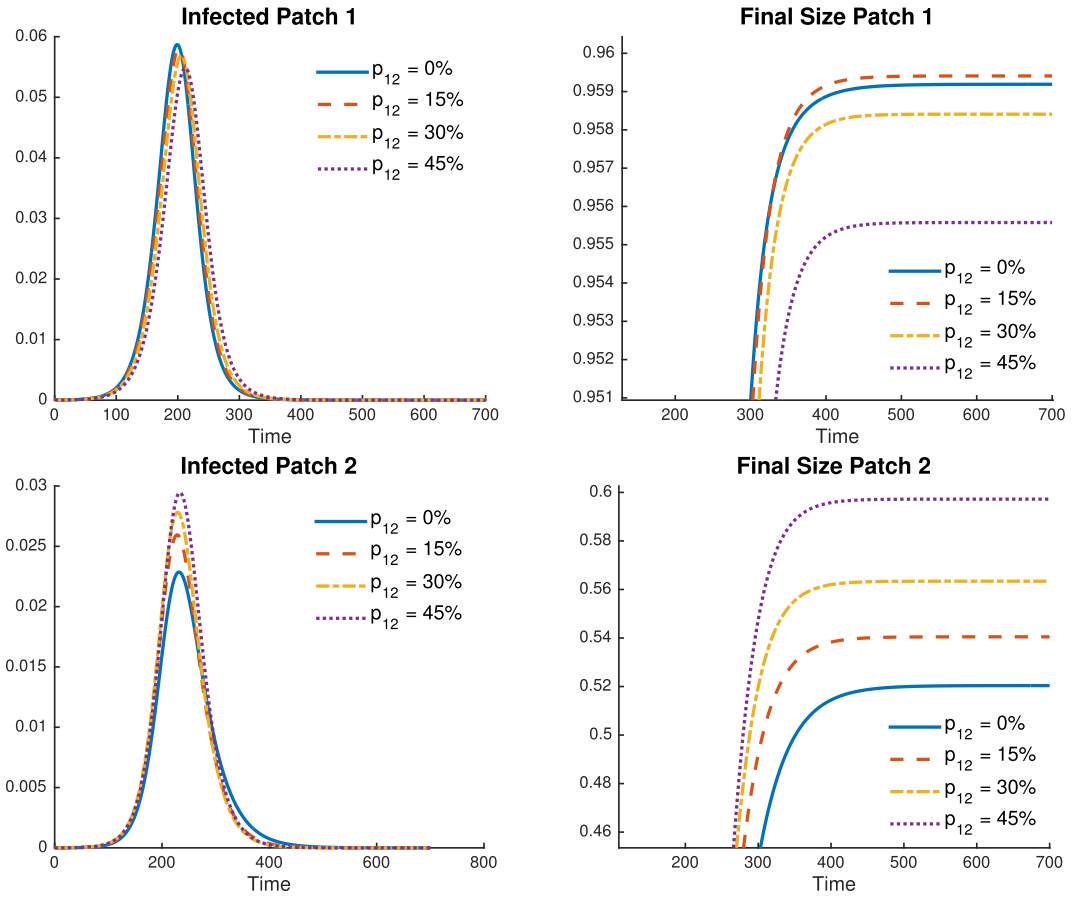

Fig. 2. Per patch incidence and final size proportions for $p_{21} = 0.10$, $p_{12} = 0, 0.15, 0.30$ and 0.45. Mobility shifts the behavior of the Patch 1 final size in the "worst case" scenario: $\mathscr{R}_{01} = 2$ and $\mathscr{R}_{02} = 0.9$.

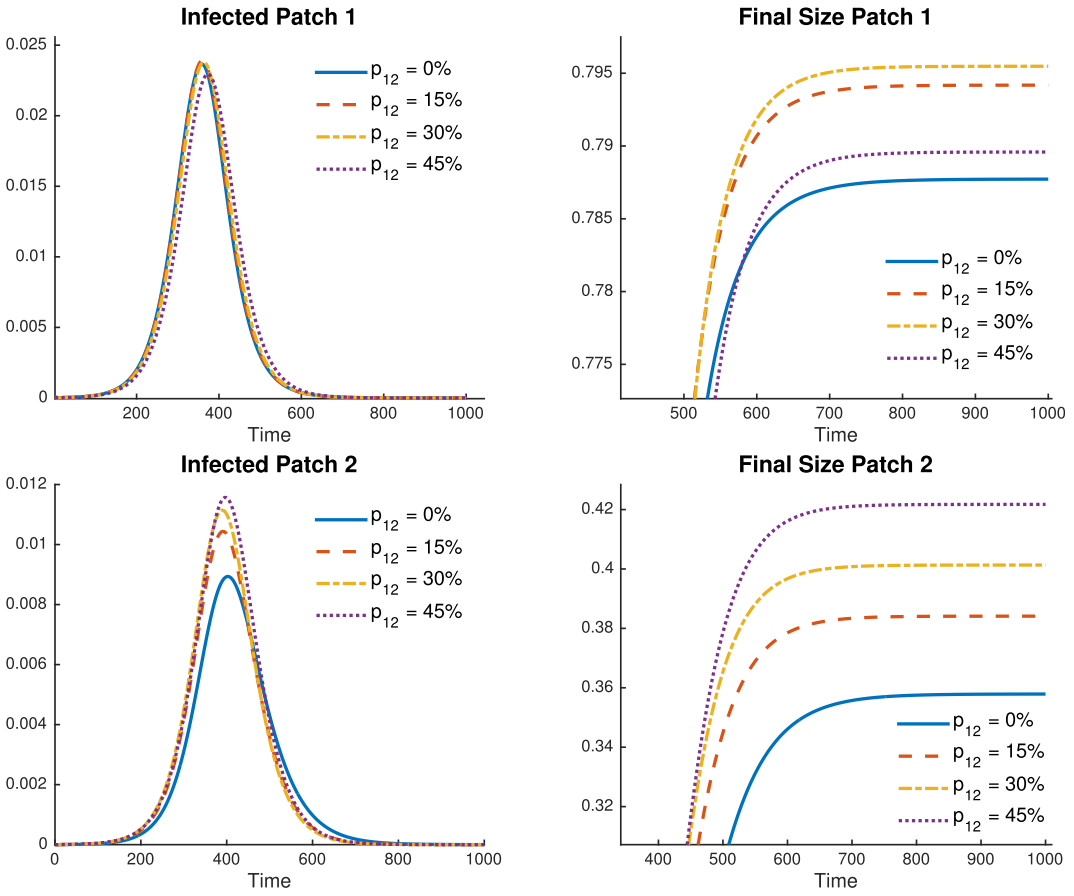

Fig. 3. Per patch incidence and final size proportions for $p_{21} = 0.10$, $p_{12} = 0, 0.15, 0.30$ and 0.45. Mobility significantly shapes the per patch final sizes in the "worst case" scenario $\mathscr{R}_{01} = 2$ and $\mathscr{R}_{02} = 0.9$.

outbreaks (Kucharski et al., 2016; Towers et al., 2016). Simulations are seeded by introducing an asymptomatic infected individual in Patch 1 under the assumption that the host and vector populations are fully susceptible in both Patches.

Fig. 2 (top), shows the incidence and final ZIKV epidemic size when Patch 1 is under the "worst case scenario," defined by a basic reproduction number of $\mathscr{R}_{01} = 2$ (Towers et al., 2016). Fig. 2 shows that at $p_{12} = 0.15$ the final number of infected residents in Patch 1 is larger to the number in the baseline scenario ($p_{12} = 0$). In fact, it reaches almost 96% of the population, an unrealistic value. Additional simulated p_{12} values show that final Patch 1 size would go below the baseline case; a benefit of mobility.

Fig. 2 highlights the case when the final Patch 2 epidemic size grows with increases in mobility when compared with the baseline case (no mobility from Patch 1). We see reductions in the final Patch 1 epidemic size for some mobility values accompanied by increments in the final Patch 2 epidemic size when compared to the baseline scenario (no mobility from Patch 1). Specifically, reductions in Patch 1 final epidemic size are around 1×10^{-3} while increments in Patch 2 are around 1×10^{-2}, under the assumption that *the population in Patch 1 is the same as that in Patch 2*. Thus while mobility may provide benefits within Patch 1 (under the above assumptions) the fact remains that it does it at a cost. In short, it is also observed that the final epidemic size per patch does not respond linearly to changes in mobility even when only the mobility p_{12} is increased (see Figs. 2 and 3).

Consider now the "best case" scenario, a basic reproductive number $\mathscr{R}_{01} = 1.52$, under the assumption that *the population in Patch 1 is the same as that in Patch 2*. The results of simulations collected in Fig. 3 show a final size epidemic curve similar to that generated in the "worst case" scenario for Patch 1. Some mobility values can increase the final Patch 1 epidemic size, reaching almost 80% of the population when $p_{12} = 0.30$, an *unrealistic* level, albeit, as expected lower than in the "worst" case scenario. The existence of a *mobility threshold* after which the final epidemic sizes in Patch 1 starts to decrease is also observed.

The results in Fig. 3 suggest that under all p_{12} mobility levels, Patch 2 final ZIKV epidemic size supports monotone growth in the total number of infected individuals. The changes in the final epidemic size in each patch in Fig. 3 are roughly equivalent (the same order, 1×10^{-2}) given that *the population in Patch 1 is the same as that in Patch 2*.

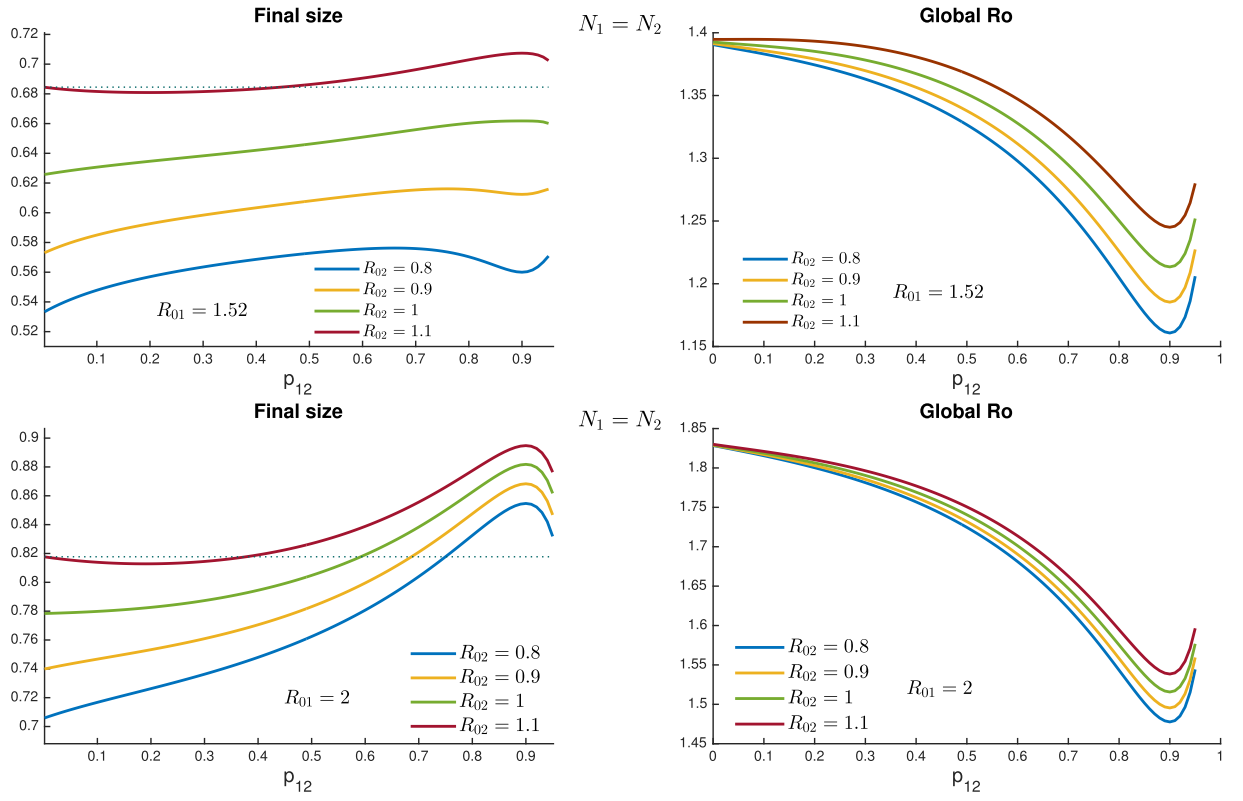

Fig. 4. Local and global final sizes through mobility values when $p_{21} = 0.10$. Although mobility reduces the global $\mathscr{R}_0$, allowing mobility in the case of El Salvador ($\mathscr{R}_0 = 2$) might lead to a detrimental effect in the global final size.

The simulation results presented so far only provide partial information on the impact that short term mobility may have on the transmission dynamics of ZIKV. This is an expected outcome given the myriad of assumptions that have been put in place, namely, the restrictions placed on population density; *the population in Patch 1 is the same as that in Patch 2*. Now, by fixing the mobility from Patch 2 to Patch 1, we are just focusing only on the impact of changes in mobility from Patch 1 to Patch 2. Further, the potential changes in mobility patterns that host populations may have in response to ZIKV dynamics are being ignored by our use of a mobility matrix $\mathbb{P}$ with constant entries p_{ij}. Yet, under such restrictions and assumptions, we have found that the qualitative response, final epidemic size within Patch 1 is qualitatively similar in the worst and best case scenarios: increasing at first, decreasing after a certain threshold and crossing down the baseline case under some mobility regimes. Further, it has been observed that the qualitative behavior of the final epidemic size in Patch 2 grows monotonically as mobility increases. Patch 1 and Patch 2 responses are of different orders of magnitude in the "worst case" scenario but roughly of the same order of magnitude in the "best case" scenario, which means, under our *restrictive conditions and assumptions*, that reductions in risk in Patch 1 do help significantly.

4.1. The role of risk heterogeneity in the dynamics of ZIKV transmission

The impact of risk heterogeneity on ZIKV dynamics within the overall two-patch system is explored, an analysis that requires the numerical estimation of the global reproduction number as a function of the mobility matrix $\mathbb{P}$. Using the previous scenarios ($\mathscr{R}_{01} = 1.52, 2$) simulations are carried out first assuming equal population sizes ($N_1 = N_2$). However, when looking at the impact of changes in risk on Patch 2 ($\mathscr{R}_{02} = 0.8, 0.9, 1, 1.1$). Our simulations identify a growing epidemic in Patch 2 as risk increases with the overall community experiencing nonlinear changes in risk as residency times change from the baseline scenario given by $p_{12} = 0$. Specifically, Fig. 4 captures overall reductions on the global reproductive number for all residence times while identifying the existence of a residence time interval for which mobility decreases the total size of the outbreak in the two patch community, when compared to the corresponding baseline case ($p_{12} = 0$).

In the absence of mobility from Patch 1 ($p_{12} = 0$), increases in the final epidemic size as $\mathscr{R}_{0i}$ increases, are observed. These simulations show that mobility can slow down the speed of the outbreak (smaller global $\mathscr{R}_0$). Of course, the simulation results also re-affirm the obvious, that is, that the existence of a high risk, mobile and well connected patch, can serve as an outbreak magnifier; a situation that has been explored within an n-patch system under various connective schemes (Bichara et al., 2015; Castillo-Chavez et al., 2016). This is because, in the two patch case, it is observed that the global reproductive

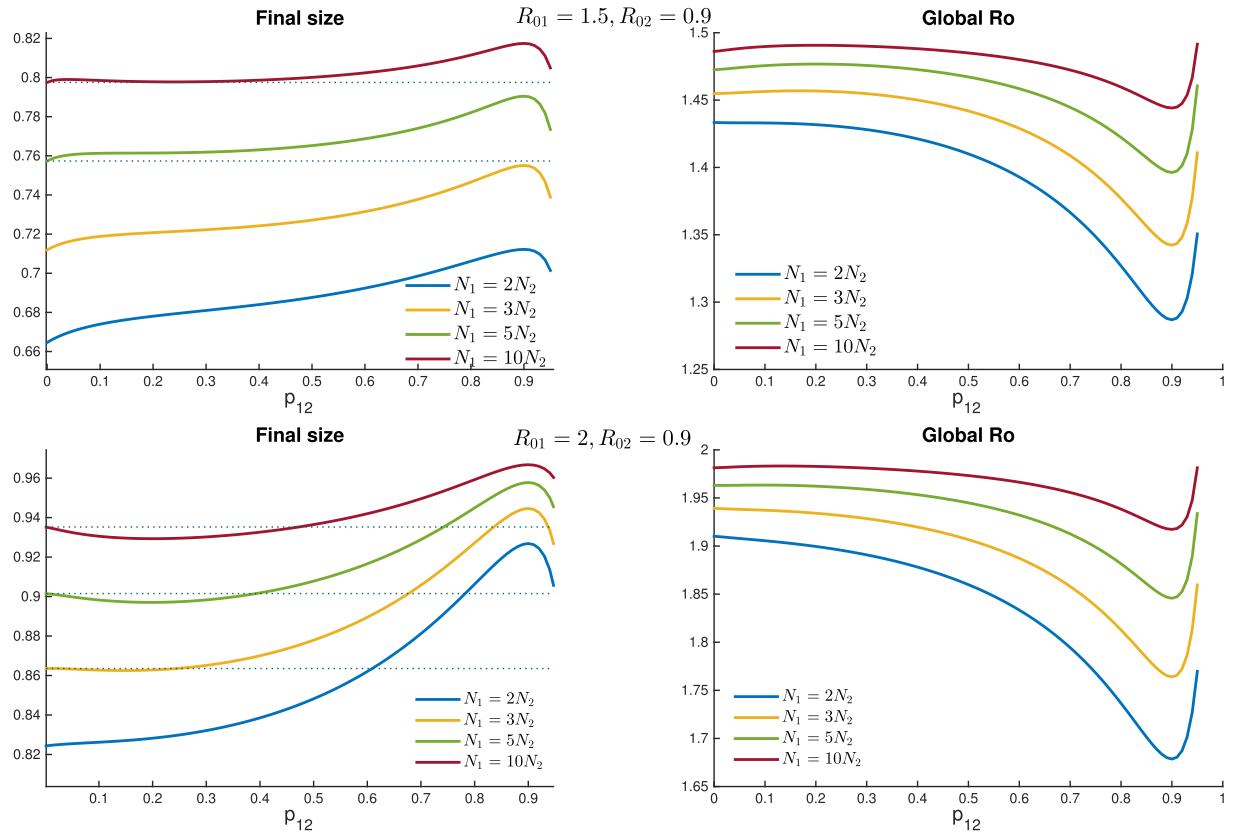

Fig. 5. Total final size and global basic reproductive number through mobility values when $p_{21} = 0.10$. Local risk values are setup to $\mathscr{R}_{02} = 0.9$ and $\mathscr{R}_{01} = 1.52, 2$.

number $\mathscr{R}_0$ experiences reductions for almost all mobility values. For the scenarios selected $\mathscr{R}_0$ never drops below 1. Hence, under our assumptions and scenarios, it is seen that the use of fixed mobility patterns make the eliminating ZIKV extremely difficult if not impossible under our two scenarios. Fig. 4 provides an example that highlights the relationship between the global reproductive number and corresponding final epidemic size.

4.2. The role of population size heterogeneity in the dynamics of ZIKV transmission

The role of population density on the total final epidemic size and global basic reproductive number are explored under our two scenarios, now under the changed assumption that the densities (population sizes) of Patch 1 and Patch 2 differ. Specifically, we take $N_1 = 2N_2$, $3N_2$, $5N_2$ and $10N_2$.

Table 2
Final size (Patch 1, Patch 2) $\mathbf{N_1 = 10000}$, $\mathscr{R}_{01} = \mathbf{2}$, $\mathscr{R}_{02} = \mathbf{0.9}$ and $\boldsymbol{p_{21}} = \mathbf{0.10}$.

N_2	Low Mobility	Intermediate Mobility	High Mobility	Min $\mathscr{R}_0$
$N_1 = N_2$	(0.9594, 0.5333)	(0.9583, 0.5633)	(0.9539, 0.6122)	1.4954
$N_1 = 2N_2$	(0.9683, 0.5418)	(0.9685, 0.5599)	(0.9667, 0.6116)	1.6786
$N_1 = 3N_2$	(0.9709, 0.5390)	(0.9713, 0.5478)	(0.9701, 0.6018)	1.7640
$N_1 = 5N_2$	(0.9729, 0.5283)	(0.9732, 0.5255)	(0.9725, 0.5852)	1.8457
$N_1 = 10N_2$	(0.9741, 0.5030)	(0.9743, 0.4908)	(0.9739, 0.5624)	1,9173

Table 3
Final size (Patch 1, Patch 2) $\mathbf{N_1 = 10000}$, $\mathscr{R}_{01} = \mathbf{1.52}$, $\mathscr{R}_{02} = \mathbf{0.9}$ and $\boldsymbol{p_{21}} = \mathbf{0.10}$.

N_2	Low mobility	Intermediate mobility	High mobility	Min $\mathscr{R}_0$
$N_1 = N_2$	(0.7920, 0.3756)	(0.7950, 0.4010)	(0.7849, 0.4304)	1.1853
$N_1 = 2N_2$	(0.8287, 0.3938)	(0.8340, 0.4061)	(0.8300, 0.4356)	1.3023
$N_1 = 3N_2$	(0.8398, 0.3948)	(0.8448, 0.3956)	(0.8422, 0.4248)	1.3590
$N_1 = 5N_2$	(0.8480, 0.3877)	(0.8520, 0.3731)	(0.8500, 0.4046)	1.4141
$N_1 = 10N_2$	(0.8533, 0.3652)	(0.8556, 0.3352)	(0.8542, 0.3756)	1.4630

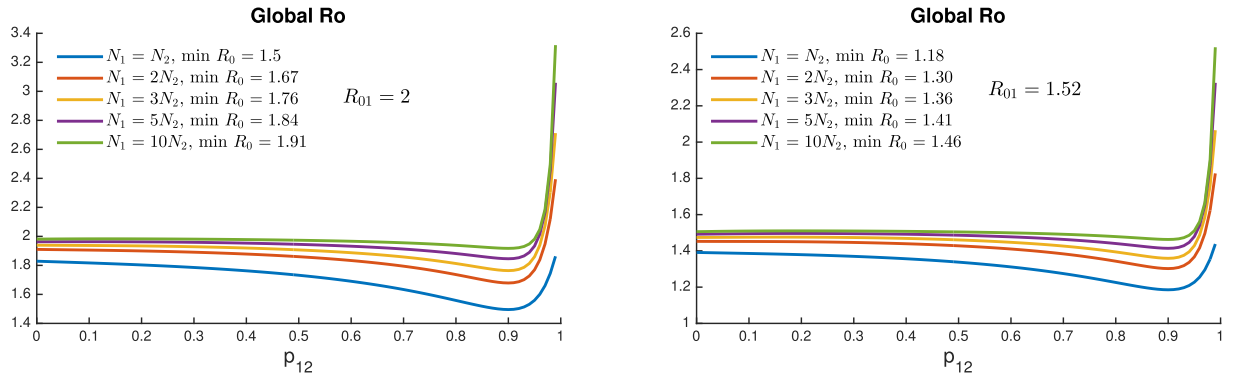

Fig. 6. Global $\mathscr{R}_0$ dynamics through mobility when $p_{21} = 0.10$. Patch 2 populations vary from $N_1 = N_2, 2N_2, 3N_2, 5N_2$ up to $N_1 = 10N_2$. The global $\mathscr{R}_0$ hits its minimum always at an unrealistic 91% of mobility. As N_1 approaches N_2, this minimum value decreases.

It is observed that difference in population sizes do matter. Specifically, it is observed that (under our selections) big difference in density indicates that a higher final epidemic size is reached. The value of 90% for the "worst case" is possible with changes in the global reproductive number exhibiting different patterns (see Fig. 5). We observe that despite increases in the total final epidemic size as mobility changes the global $\mathscr{R}_0$ actually decreases monotonically for most residence times, never falling bellow one. A sensible degree of magnification on the spread of the disease as residence times change is observed whenever the differences between N_1 and N_2 are not too extreme. In fact, it is possible for mobility to be beneficial in the control of ZIKV under the above simplistic extreme scenarios. Simulations continue to show that under the prescribed conditions and assumptions, model generated ZIKV outbreaks remain unrealistically high.

The simulations show, for example, that the global reproductive number reaches its minimum at around $p_{12} = 0.90$ with Fig. 5 showing that the larger the high risk population gets ($N_1 \gg N_2$), the greater the total final epidemic size becomes as individuals from Patch 1 spend more than half of their day in Patch 2. Using a low p_{12} value, a small benefit is observed, namely, the total final epidemic size is reduced, when the differences between $\mathscr{R}_{0i}$ are high.

For the two epidemiological scenarios $\mathscr{R}_{01} = 2$ and $\mathscr{R}_{01} = 1.52$, Tables 2 and 3 provide a summary of the average proportion of infected for low ($p_{12} = 0 - 0.2$), intermediate ($p_{12} = 0.2 - 0.4$) and high mobility ($p_{12} = 0.4 - 0.6$) when $p_{21} = 0.10$. The role of population scaling $N_1 = 2N_2$, $3N_2$, $5N_2$ and $10N_2$ is also explored.

Fig. 6 shows the global $\mathscr{R}_0$ over all mobility values for different population weights in the two epidemic scenarios. The minimum $\mathscr{R}_0$ value is reached for all cases when mobility is at an unrealistic 91% and when $N_1 \approx N_2$.

The results collected in Fig. 6 show that short-term mobility plays an important role in ZIKV dynamics, again, under a system involving two highly differentiated patches. Simulations also suggest that, even though mobility can reduce the global basic reproductive number, that is not enough to eliminate an outbreak or really make a difference under our two scenarios.

5. Conclusions and discussion

A two-patch model where host-mobility is modeled using a Lagrangian approach is used to help understand the role of host-movement on the transmission dynamics of ZIKV. This study focuses on the dynamics of a single outbreak albeit the modeling framework can be used to study long-term dynamics as well, as long as the mobility patterns can be captured effectively by the matrix $\mathbb{P}$; which seems to be appropriate when used to model, for example, daily activity patterns within an urban center. We make use of only two patches, *as distinct as they can be*, with the hope that simulations in this simplified system can shed some light on the transmission dynamics of ZIKV, in the presence of extreme health disparities within neighboring communities or within urban centers. This framework can be used to study the dynamics of vector born diseases within a collection of neighboring communities or neighborhoods experiencing multiple levels of health disparities and diverse connectivity mobility structures (Bichara & Castillo-Chavez, 2016). The study of the role of mobility at larger scales can be best captured using question-specific related models that account for the possibility of long-term mobility (see for example (Banks and Castillo-Chavez, 2003; Baroyan et al., 1971; Chowell, Hyman, Eubank, & Castillo-Chavez, 2003b; Elveback et al., 1976; Herrera-Valdez, Cruz-Aponte, & Castillo-Chavez, 2011; Khan et al., 2009; Rvachev & Longini, 1985)).

Although the goal is not to fit specific outbreaks or specific situations, we still make use of recently published parameter ranges, including some reported by us (Towers et al., 2016); since framing the system within the range of ZIKV accepted parameters helps highlight the impact that mobility may have within two highly distinct (bi-modal) communities. The introduction of a Lagrangian modeling approach to study epidemic ZIKV outbreaks is also useful as it makes use of *measurable* parameters, for instance risk ($\widehat{\beta}$), which affect individuals differentially as a function of measurable patch-residency times and, of course, mobility patterns (residency times).

The impact of ZIKV can be assessed locally (each patch) or globally, that is, over the two patch system. System risk assessment was carried out via the computation of the system $\mathscr{R}_0$, which must be carried out via the numerical solution of a system of nonlinear equations. Specifically, changes on the system $\mathscr{R}_0$ were computed (as residency times were varied) in relationship to the local $\mathscr{R}_{0i}$, that is, *local* basic reproduction numbers, both computed in the absence of mobility. Further, the mobility-dependent system final epidemic sizes were computed via simulations that helped asses the impact of mobility (and risk) not only locally but also on the overall system; an evaluation that depends on estimates of the overall basic reproduction number (a measure of the disease's short-term power and long-term impact). The metrics used in our assessment include the overall final epidemic size (a measure of the overall impact of an outbreak), a function of mobility within the two selected scenarios, ($\mathscr{R}_{01} = 1.52$ and $\mathscr{R}_{01} = 2$).

It was found out that mobility's impact on the total final epidemic size depends on the local risk of infection and patch population size. It was also determined that short term mobility is not always beneficial (hence the importance of reducing health disparities at the most vulnerable places). In fact, mobility from high to low risk patches can reduce or increase the total final epidemic size.

The challenges posed by policies that may be beneficial to the system but detrimental are also explored within our two-patch system. Situations where the total final epidemic size increased with R_{02} increases and situations where the total final epidemic size decreased under low mobility values when $R_{02} > 1$ were documented. Population density does make a difference and examples when $R_{02} < 1$ with mobility incapable of reducing the total final epidemic size under no differences in patch density (here measured by total population size in each patch, both assumed to have roughly the same area) were also identified. Differences in population density were also shown to be capable of generating reductions on the total final epidemic size within some mobility regimes.

The highly simplified two-patch model used seem to have shed some light on the role of mobility on the spread of ZIKV in areas where huge differences in the availability of public health programs and services —the result of endemic crime, generalized violence and neglect— exist. Model simulations also seemed to have shed some light on the potential relevance of the factors that we failed to account for. The value of the use of single patch-specific risk parameters ($\widehat{\beta}$) has strengths and limitations. It is important to notice that the model used did not account explicitly for changes in the levels of infection within the vector population nor does it account for impact of substantial differences in patch vector population sizes. The simplified model fails to account for the responses to outbreaks by patch residents as individuals may alter mobility patterns, use more protective clothing, and respond individually and independently of official control programs in response to dramatic increases on vector population or a surge in cases. Clearly, the use of two patches and our assumptions do limit the outcomes that such a system can support. Communities can't in generally be modeled under a highly differentiated two-tier system and in the case of ZIKV, the possibility of vertical transmission in humans and vectors as well as sexually-transmitted ZIV can't be completely neglected (Brauer, Castillo-Chavez, Mubayi, & Towers, 2016). The introduction of changes in behavior in response to individuals' assessment of the levels of risk infection over time needs to be addressed (Castillo-Chavez et al., 2016); a challenge that has yet to be met to the satisfaction of the scientific community involved in the study of epidemiological processes as complex adaptive systems (see for example (Fenichel et al., 2011; Morin, Fenichel, & Castillo-Chavez, 2013; Perrings et al., 2014)).

The limitations of the role of technology in the absence of the public health infrastructure —there is no silver bullet— has been recently addressed in the context of Ebola ((Chowell et al., 2015; Yong, Herrera, & Castillo-Chavez, 2016)) with applications of the Lagrangian approach as presented here in the context of communicable and vector born diseases, including dengue, tuberculosis and Ebola, in settings where health disparities are pervasive ((Bichara et al., 2016; Espinoza et al., 2016, p. pp.123)). Further, the use of simplified models, quite often tends to over-estimate the impact of an outbreak (see (Nishiura et al., 2009, 2011)) and the model and scenarios used highlight the limitations on the use of simplified settings when the goal is to capture or mimic the dynamics of specific systems—not the goal of this manuscript.

Certainly, we have seen the use of dramatic measures to limit the spread of diseases like SARS, Influenza or Ebola ((Chowell et al., 2003a, 2015; Herrera-Valdez et al., 2011)), as well as the rise of vector born diseases like Dengue and Zika, and the dramatic implications that some measures have had on local and global economies. The question remains, what can we do to mitigate or limit the spread of disease, particularly emergent diseases without disrupting central components? Discussions on these issues are recurrent (Fenichel et al., 2011; Morin et al., 2013), most intensely in the context of SARS, Influenza, Ebola and Zika, in the last decade or so. The vulnerability of world societies is directly linked to the lack of action in addressing the challenges faced by the weakest links in the system must be accepted and acted on by the world community. We need global investments in communities and nations where health disparities and lack of resources are the norm. We must invest in research and surveillance within clearly identified world hot spots, where the emergence of new disease are most likely to emerge, and we must do so with the involvement, at all levels, of the affected communities (Castillo-Chavez et al., 2015; Perrings et al., 2014).

Acknowledgements

This paper is dedicated to the inauguration of the Centro de Modelamiento Matemático Carlos Castillo-Chávez at Universidad Francisco Gavidia in San Salvador, El Salvador.

This project has been partially supported by grants from the National Science Foundation (DMS-1263374 and DUE-1101782), the National Security Agency (H98230-14-1-0157), the Office of the President of ASU, and the Office of the Provost of ASU. The views expressed are sole responsibility of the authors and not the funding agencies.

References

Banks, H. T., & Castillo-Chavez, C. (2003). Bioterrorism: Mathematical modeling applications in homeland security. *SIAM, 28*.
Baroyan, O. V., Rvachev, L. A., Basilevsky, U. V., Ermakov, V. V., Frank, K. D., Rvachev, M. A., et al. (1971). Computer modelling of influenza epidemics for the whole country (USSR). *Advances in Applied Probability, 3*, 224–226.
Bichara, D., & Castillo-Chavez, C. (2016). Vector-borne diseases models with residence times–a lagrangian perspective. *Mathematical Biosciences, 281*, 128–138.
Bichara, D., Holechek, S. A., Velazquez-Castro, J., Murillo, A. L., & Castillo-Chavez, C. (2016). On the dynamics of dengue virus type 2 with residence times and vertical transmission. *Letters in Biomathematics, 3*(1), 140–160.
Bichara, D., Kang, Y., Castillo-Chavez, C., Horan, R., & Perrings, C. (2015). Sis and sir epidemic models under virtual dispersal. *Bulletin of mathematical biology, 77*, 2004–2034.
Brauer, F., & Castillo-Chavez, C. (2012). *Mathematical models in population biology and epidemiology* (Vol. 40). Springer.
Brauer, F., Castillo-Chavez, C., Mubayi, A., & Towers, S. (October 2016). Some models for epidemics of vector-transmitted diseases. *Infectious Disease Modelling, 1*(1), 79–87.
Cao-Lormeau, V.-M., & Musso, D. (2014). Emerging arboviruses in the pacific. *The Lancet, 384*, 1571–1572.
Cao-Lormeau, V. M., Roche, C., Teissier, A., Robin, E., Bery, A.-L., Mallet, H.-P., et al. (2014). *Zika virus, French Polynesia, south pacific, 2013*.
Castillo-Chavez, C., Barley, K., Bichara, D., Chowell, D., Herrera, E. D., Espinoza, B., et al. (2016). Modeling ebola at the mathematical and theoretical biology institute (MTBI). *Notices of the AMS, 63*.
Castillo-Chavez, C., Curtiss, R., Daszak, P., Levin, S., Patterson-Lomba, O., Perrings, C., et al. (2015). Beyond Ebola: Lessons to mitigate future pandemics. *The Lancet Global Health, 3*, e354–e355.
CDC(a). (2016). *Zika virus*. Online, February 18, 2016.
CDC(b). (February 2016). *CDC adds 2 destinations to interim travel guidance related to zika virus*. Online.
CDC(c). (February 2016). *Zika virus in South America*. Online.
CDC(d). (February 2016). *Zika virus in Central America*. Online.
CDC(f). (October 2016). *All countries & territories with active zika virus transmission*. Online.
Chowell, D., Castillo-Chavez, C., Krishna, S., Qiu, X., & Anderson, K. S. (2015). Modelling the effect of early detection of Ebola. *The Lancet Infectious Diseases, 15*, 148–149.
Chowell, G., Fenimore, P. W., Castillo-Garsow, M. A., & Castillo-Chavez, C. (2003). SARS outbreaks in Ontario, Hong Kong and Singapore: The role of diagnosis and isolation as a control mechanism. *Journal of Theoretical Biology, 224*, 1–8.
Chowell, G., Hyman, J. M., Eubank, S., & Castillo-Chavez, C. (2003). Scaling laws for the movement of people between locations in a large city. *Physical Review E, 68*, 066102.
Dick, G., Kitchen, S., & Haddow, A. (1952). Zika virus (i). isolations and serological specificity. *Transactions of the Royal Society of Tropical Medicine and Hygiene, 46*, 509–520.
Duffy, M. R., Chen, T.-H., Hancock, W. T., Powers, A. M., Kool, J. L., Lanciotti, R. S., et al. (2009). Zika virus outbreak on yap island, Federated States OF Micronesia. *New England Journal of Medicine, 360*, 2536–2543.
Dupont-Rouzeyrol, M., O'Connor, O., Calvez, E., Daures, M., John, M., Grangeon, J.-P., et al. (2015). Co-infection with zika and dengue viruses in 2 patients, New Caledonia, 2014. *Emerging infectious diseases, 21*, 381.
Elveback, L. R., Fox, J. P., Ackerman, E., Langworthy, A., Boyd, M., & Gatewood, L. (1976). An influenza simulation model for immunization studies. *American Journal of Epidemiology, 103*, 152–165.
Espinoza, B., Moreno, V., Bichara, D., & Castillo-Chavez, C. (2016). Assessing the efficiency of movement restriction as a control strategy of ebola. *Mathematical and Statistical Modeling for Emerging and Re-emerging Infectious Diseases*, pp.123–145.
Fauci, A. S., & Morens, D. M. (2016). Zika virus in the americas—yet another arbovirus threat. *New England Journal of Medicine, 374*(7), 601–604.
Faye, O., Freire, C. C., Iamarino, A., Faye, O., de Oliveira, J. V. C., Diallo, M., et al. (2014). Molecular evolution of zika virus during its emergence in the 20th century. *PLoS Negl Trop Dis, 8*, e2636.
Fenichel, E. P., Castillo-Chavez, C., Ceddia, M. G., Chowell, G., Gerardo, Parra, P. A. G., et al. (2011). Adaptive human behavior in epidemiological models. *Proceedings of the National Academy of Sciences, 108*, 6306–6311.
Gazette, H. (October 2016). *Paper disc can quickly detect Zika virus in the field*. Online.
Haddow, A. D., Schuh, A. J., Yasuda, C. Y., Kasper, M. R., Heang, V., Huy, R., et al. (2012). Genetic characterization of zika virus strains: Geographic expansion of the asian lineage. *PLoS Negl Trop Dis, 6*, e1477.
Hayes, E. B., et al. (2009). Zika virus outside africa. *Emerging Infectious Diseases, 15*, 1347–1350.
Herrera-Valdez, M. A., Cruz-Aponte, M., & Castillo-Chavez, C. (2011). Multiple outbreaks for the same pandemic: Local transportation and social distancing explain the different ?waves? of A-H1N1pdm cases observed in Mexico during 2009. *Mathematical Biosciences and Engineering, 8*, 21–48.
Jaitman, L. (2015). *Los costos del crimen y la violencia en el bienestar en America Latina y el Caribe, Laura Jaitman Ed., Banco Interamericano del Desarrollo*.
Khan, K., Arino, J., Hu, W., Raposo, P., Sears, J., Calderon, F., et al. (2009). Spread of a novel influenza A (H1N1) virus via global airline transportation. *New England journal of medicine, 361*, 212–214.
Kucharski, A. J., Funk, S., Eggo, R. M., Mallet, H.-P., Edmunds, J., & Nilles, E. J. (2016). Transmission dynamics of zika virus in island populations: A modelling analysis of the 2013-14 French Polynesia outbreak. *bioRxiv*, 038588.
Lee, S., & Castillo-Chavez, C. (2015). The role of residence times in two-patch dengue transmission dynamics and optimal strategies. *Journal of theoretical biology, 374*, 152–164.
Macnamara, F. (1954). Zika virus: A report on three cases of human infection during an epidemic of jaundice in Nigeria. *Transactions of the Royal Society of Tropical Medicine and Hygiene, 48*, 139–145.
Morin, B., Fenichel, E. P., & Castillo-Chavez, C. (2013). SIR dynamics with economically driven contact rates. *Natural resource modeling, 26*, 505–525.
Musso, D., Cao-Lormeau, V. M., & Gubler, D. J. (2015). Zika virus: Following the path of dengue and chikungunya? *The Lancet, 386*, 243–244.
Musso, D., Nilles, E., & Cao-Lormeau, V.-M. (2014). Rapid spread of emerging zika virus in the pacific area. *Clinical Microbiology and Infection, 20*, O595–O596.
Nishiura, H., Castillo-Chavez, C., Safan, M., Chowell, G., et al. (2009). Transmission potential of the new influenza A (H1N1) virus and its age-specificity in Japan. *Euro Surveill, 14*, 19227.
Nishiura, H., Chowell, G., & Castillo-Chavez, C. (2011). Did modeling overestimate the transmission potential of pandemic (H1N1-2009)? Sample size estimation for post-epidemic seroepidemiological studies. *Plos one, 6*, e17908.
Patterson-Lomba, O., Goldstein, E., Gómez-Liévano, A., Castillo-Chavez, C., & Towers, S. (2015). Per capita incidence of sexually transmitted infections increases systematically with urban population size: A cross-sectional study. *Sexually Transmitted Infections*. http://dx.doi.org/10.1136/sextrans-2014-051932. pp. sextrans–2014.
Patterson-Lomba, O., Safan, M., Towers, S., & Taylor, J. (2016). Modeling the role of healthcare access inequalities in epidemic outcomes. *Mathematical Biosciences and Engineering, 13*, pp.1011–1041.

Perrings, C., Castillo-Chavez, C., Chowell, G., Daszak, P., Fenichel, E. P., Finnoff, D., et al. (2014). Merging economics and epidemiology to improve the prediction and management of infectious disease. *EcoHealth, 11*, 464–475.
Petersen, E. E. (2016). Interim guidelines for pregnant women during a zika virus outbreak—United States, 2016. *MMWR. Morbidity and mortality weekly report, 65*.
Rvachev, L. A., & Longini, I. M. (1985). A mathematical model for the global spread of influenza. *Mathematical biosciences, 75*, 322.
Salvador, F. S., & Fujita, D. M. (2015). *Entry routes for zika virus in Brazil after 2014 world cup: New possibilities, Travel medicine and infectious disease*.
Stroud, P., Del Valle, S., Sydoriak, S., Riese, J., & Mniszewski, S. (2007). Spatial dynamics of pandemic influenza in a massive artificial society. *Journal of Artificial Societies and Social Simulation, 10*.
The Biodesign Institute. (October 2016). *Green named Health Care Hero finalist for Zika virus detection device*. Online.
Towers, S., Brauer, F., Castillo-Chavez, C., Falconar, A. K., Mubayi, A., & Romero-Vivas, C. M. E. (December 2016). Estimation of the reproduction number of the 2015 zika virus outbreak in barranquilla, Colombia, and estimation of the relative role of sexual transmission. *Epidemics, 17*, 50–55.
W. H. O. (WHO). (January 2016). *Zika virus, fact sheet*. Online.
Yong, K. E., Herrera, E. D., & Castillo-Chavez, C. (2016). From bee species aggregation to models of disease avoidance: The\ emph {Ben-Hur} effect. *Mathematical and Statistical Modeling for Emerging and Re-emerging Infectious Diseases, 63*, 169–185.
Zanluca, C., Melo, V. C. A. D., Mosimann, A. L. P., Santos, G. I. V. d., Santos, C. N. D. d., & Luz, K. (2015). First report of autochthonous transmission of zika virus in Brazil. *Memórias do Instituto Oswaldo Cruz, 110*, 569–572.
Zhao, H., Feng, Z., & Castillo-Chavez, C. (2014). The dynamics of poverty and crime. *Journal of Shanghai Normal University (Natural Sciences Mathematics), 43*(5), 486–495.
Online, February 01, 2016. *Zika virus* (2016.